

Measurement of the space charge effect of a negative hydrogen ion beam

T. Bykov, D. Kasatov, Ia. Kolesnikov, A. Koshkarev, A. Makarov, Yu. Ostreinov, I. Shchudlo, E. Sokolova, I. Sorokin, and S. Taskaev

Citation: *AIP Conference Proceedings* **2052**, 070004 (2018); doi: 10.1063/1.5083784

View online: <https://doi.org/10.1063/1.5083784>

View Table of Contents: <http://aip.scitation.org/toc/apc/2052/1>

Published by the *American Institute of Physics*

AIP | Conference Proceedings

Get **30% off** all
print proceedings!

Enter Promotion Code **PDF30** at checkout



Measurement of the Space Charge Effect of a Negative Hydrogen Ion Beam

T. Bykov^{1,2}, D. Kasatov^{1,2}, Ia. Kolesnikov^{1,2, a)}, A. Koshkarev^{1,2}, A. Makarov^{1,2},
Yu. Ostreinov^{1,2}, I. Shchudlo^{1,2}, E. Sokolova^{1,2}, I. Sorokin^{1,2}, S. Taskaev^{1,2, b)}

¹ *Budker Institute of Nuclear Physics, Novosibirsk, Russia*

² *Novosibirsk State University, Novosibirsk, Russia*

a) Corresponding author: katyono@mail.ru

b) taskaev@inp.nsk.su

Abstract. A source of epithermal neutrons based on a vacuum-insulated tandem accelerator and a lithium target is developed for the technique of boron neutron capture therapy. A 2 MeV stationary proton beam with a current of up to 5 mA was obtained in the accelerator. With a view of increasing the current, the transport of a beam of negative hydrogen ions from the ion source to the accelerator is studied using a wire scanner OWS-30 (D-Pace, Canada) and a movable diaphragm. Dependences of the ion beam profile and the current on the residual gas pressure are measured and the influence of the space charge is detected. We measured the phase portrait of the beam in the radial and azimuth directions and discovered the effect produced by the aberrations of the focusing magnetic lens. We also gaged the value of the normalized beam emittance. The change in beam focusing mode and the introduction of optical diagnostics of the beam position in the diaphragm of the first accelerating electrode made it possible to significantly improve the stability of the accelerator operation at high current of the proton beam, up to 6.7 mA.

INTRODUCTION

An accelerating source of epithermal neutrons was proposed and created at the Budker Institute of Nuclear Physics [1,2] for the further development of a promising technique for the treatment of malignant tumors - boron neutron capture therapy (BNCT) [3]. Neutron generation results from ${}^7\text{Li}(p,n){}^7\text{Be}$ threshold reaction initiated by directing a 2-MeV proton beam with a current of up to 5 mA produced in a vacuum-insulated tandem accelerator [2, 4] to a 10-cm diameter lithium target [5]. In the paper, the transport of a beam of negative hydrogen ions from the ion source to the accelerator is studied using a wire scanner and a movable diaphragm. The study is necessary due to the consequences that are manifested when the current of negative hydrogen ions was injected into the accelerator increases. First, with increasing injection current for stable operation of the accelerator it was required to change the force of the magnetic lens focusing the beam of negative hydrogen ions to the entrance of the accelerator. Secondly, as the injection current increased the frequency of high voltage breakdowns increased. Thirdly, when the injection current was increased the diaphragms of the accelerating electrodes are heated up to 1000 °C. It was necessary to find out the reasons for these phenomena before replacing the source of negative hydrogen ions with a new one with a high current and obtaining a beam of protons with a current of more than 10 mA. If a proton beam with a current of 10 mA is obtained in such a compact accelerator as a tandem accelerator with vacuum isolation, it will help to create a compact source of epithermal neutrons for BNCT.

EXPERIMENTAL SETUP

Figure 1 schematically shows a fragment of the experimental facility used in these experiments. Negative hydrogen ions with an energy of 22 keV are generated by a surface plasma source 1 using the Penning discharge with hollow cathodes. The beam of negative hydrogen ions leaving the source rotates through an angle of 15° in the source magnetic field, passes through the aperture of a conical diaphragm with a diameter of 28 mm (2), is focused by a pair of magnetic lenses 5 and is injected into the vacuum-insulated tandem accelerator. The gas is pumped out by two turbomolecular pumps TMP-3203lm (Shimadzu, Japan) 4 and 13 at a hydrogen pumping rate of 2400 l/s. The residual gas pressure is regulated by the leak valve 12 added for this experiment. The residual gas pressure is measured by a vacuum lamp Pfeiffer vacuum d-35614 3.

The current and profile of the negative hydrogen ion beam injected into the accelerator are measured by the wire scanner OWS-30 (D-Pace, Canada; under the license of TRIUMF) [6] 7 placed before the cooled diaphragm 8. The scanner was also used to measure the current profile of the ion beam when, at a distance of 225 mm, a diaphragm made from a 1 mm thick tantalum plate with a 0.8 mm diameter opening was introduced into the beam. The opening was countersunk on the both sides of the plate. Moving the diaphragm at an angle of 45° to the axis of the scanner (along the y axis, see Fig. 2) made it possible to measure the phase portrait of the beam in the radial and azimuthal directions and to determine the emittance of the beam.

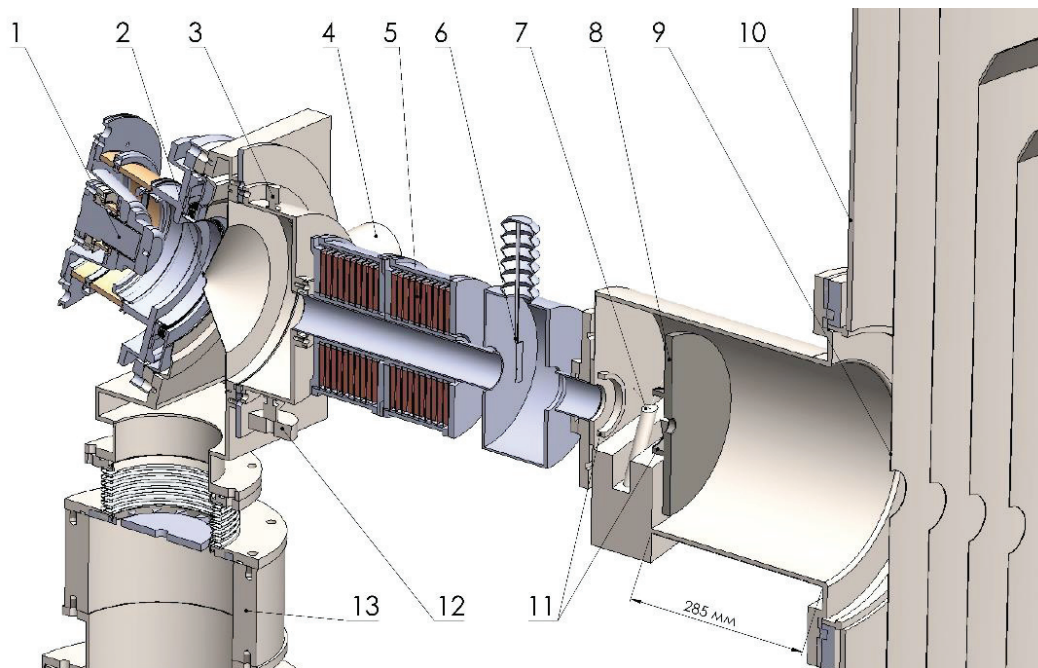


FIGURE 1. Experimental facility: 1 – source of H^- ions, 2 – conical diaphragm, 3 – vacuum lamp, 4 and 13 – turbomolecular pumps, 5 – magnetic lenses, 6 – movable diaphragm, 7 – wire scanner OWS-30, 8 – cooled diaphragm, 9 – first electrode of the accelerator, 10 – vacuum tank of the accelerator, 11 – metal rings, 12 – leak valve.

Preparation of the OWS-30 Wire Scanner for the Experiments

Scheme of the OWS-30 wire scanner is shown on the Fig. 2. In the scanner, there are two orthogonal tungsten wires 0.5 mm in diameter, 49 mm long and fixed on a common rod, which is deflected from the axis crossing the center of the ion beam by an angle of 13.5° , and when it is used for measuring, it rotates to an angle of -13.5° and comes back. The rotation axis of the rod is at a distance of 190 mm from the center of the ion beam. When the rod moves, the current is measured (with an accuracy of $10^{-10}A$) as well as the deflection angle of the rod; these values with the beam diameter less than 30 mm allow one to reconstruct the transverse profile of chordal measurements of the ion beam current in two orthogonal planes and to determine the value of the total current [7].

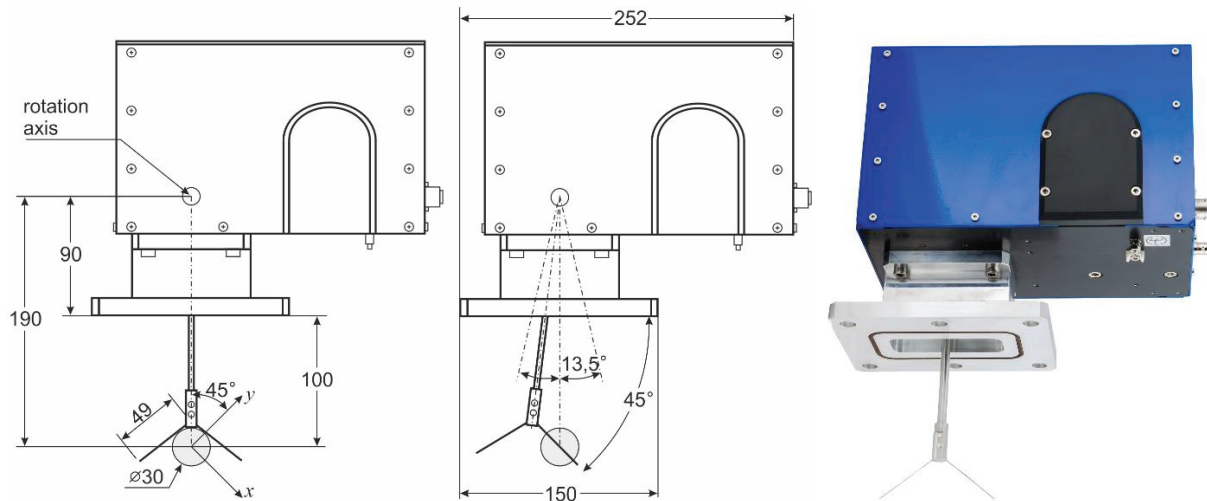


FIGURE 2. Scheme (left) and photo (right) of the OWS-30 wire scanner. In addition, the ion beam (a circle with a diameter of 30 mm) and the coordinate system (x, y) , which is used later in the text when presenting the results, are shown.

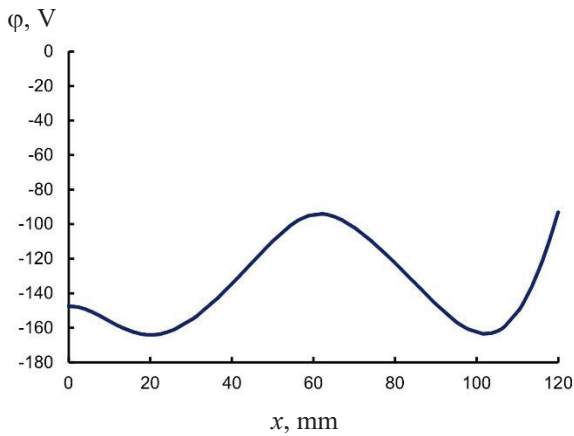


FIGURE 3. The distribution of the electric field potential along the transport line axis. The scanner coordinate is 60 mm; the ion source is to the left of this coordinate, and the accelerator is to the right.

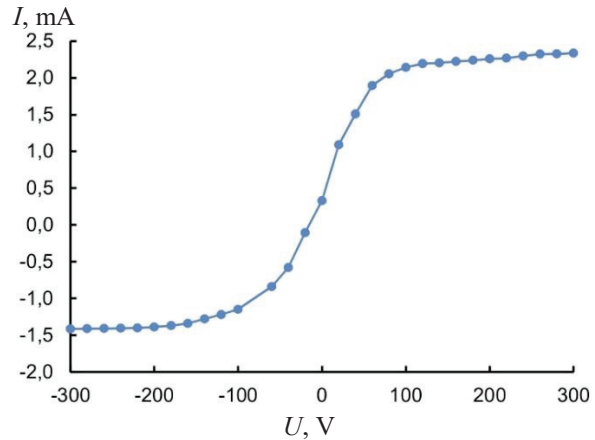


FIGURE 4. The dependence of the current I measured by the OWS-30 scanner on the potential of the metal rings U .

Due to the secondary electrons emission signals of the OWS-30 wire scanner were positive. To correctly measure the ion current, the scanner was upgraded: one metal ring II with an inner diameter of 60 mm was installed both in front of the scanner and past it at distances of about 40 mm. Each ring was kept at a negative potential of 300 V to suppress the secondary emission of electrons from the scanner wires. The calculated potential of the electric field along the axis of the transport channel is shown in Fig. 3. It can be seen that a potential barrier with a height of 160 V is created for electrons emitted from the scanner wires. Fig. 4 shows the dependence of the current of the charged-particle beam measured by the wire scanner on the potential of the rings. A potential of -300 V is sufficient to suppress the secondary emission of electrons.

An additional software for the OWS-30 wire scanner was created. It calculates total current, size of the beam, destination relatively to an axis of the accelerator and show approximation of the beam's profile. Detailed information written in a paper [8].

MEASUREMENT RESULTS AND DISCUSSION

Figure 5 shows the graphs of the current, cross-sectional area, and current density of the negative hydrogen ion beam versus the pressure of the residual gas regulated by the leak valve. Here, the cross-sectional area is understood as a quantity calculated by the formula of ellipse area where each side of the ellipse is equal to the width, the current area under which is 95% of the total current.

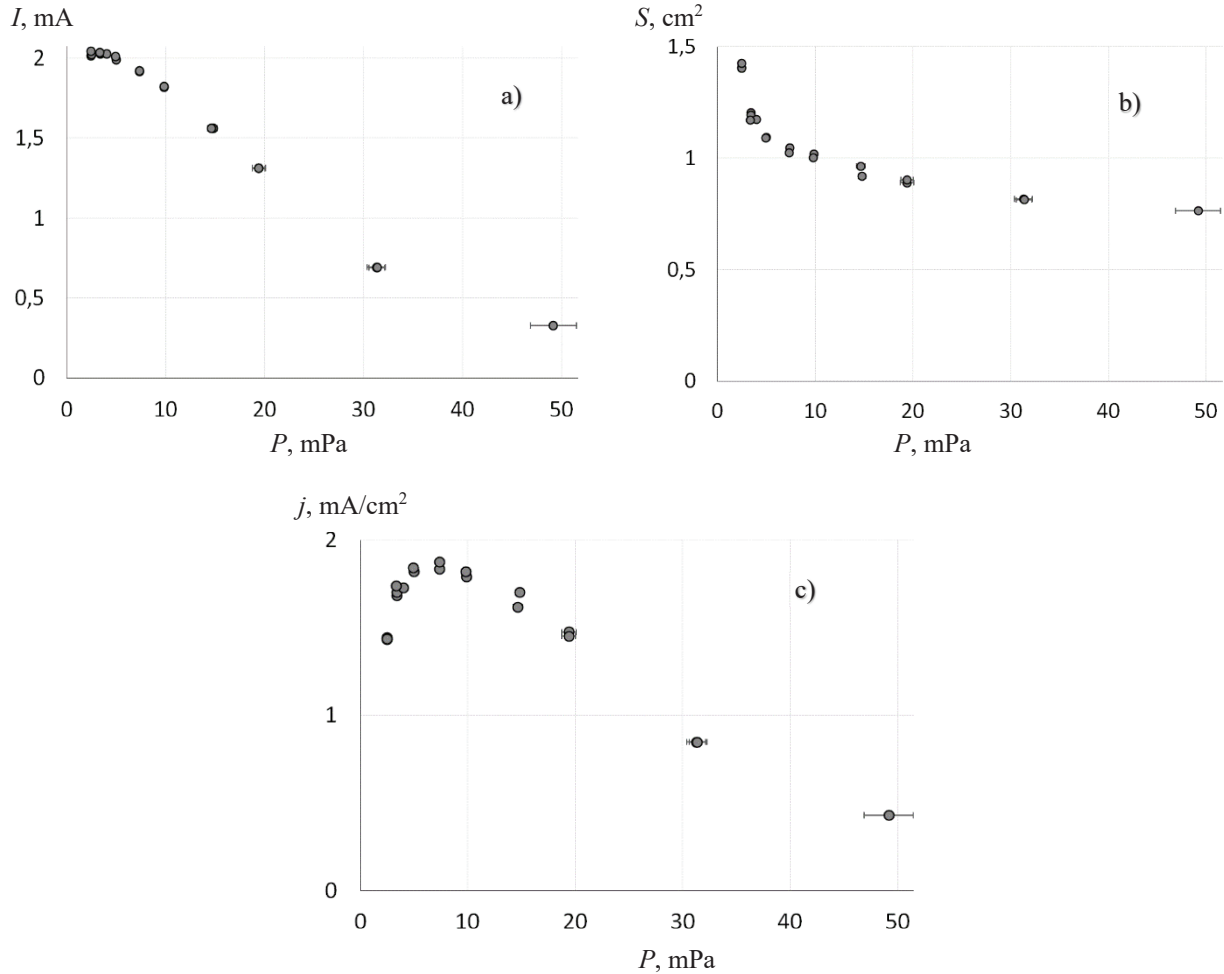


FIGURE 5. Beam current I (a), cross section area S (b) and H^- beam current density j (c) vs the residual gas pressure P

It is seen that the deterioration in the vacuum conditions is accompanied not only by the ion current decrease, which is due to ion stripping on the residual gas but also by the reduction in the beam size, which can be attributed to the weakening of the ion space charge. The maximum ion current density is attained not under the best vacuum conditions, but at a residual gas pressure of 7.4 ± 0.2 mPa. When the vacuum is improved to the best level of 2.5 ± 0.1 mPa, the ion beam current increases by 5 %, and its size grows by 36%, so that the current density decreases by 25 %. Thus, it became clear that there was no need to improve the gas pumping out in the beam transport path. The optimal beam input is realized at some residual gas pressure, in this case 7.4 mPa, sufficiently small for minor stripping of the ion beam and large enough to compensate for the space charge effect. The injection of a negative hydrogen ion beam into an accelerator with a maximum current density is important for the stable operation of the accelerator since the small aperture of the cooled diaphragm (δ in Fig. 1) is able to reduce the undesirable penetration of hydrogen being pumped into the ion source and other particles into the accelerator.

Figure 6 presents profiles of chordal measurements of the ion current and reconstructed radial current distributions. The data presented in Fig. 6a is the dependence of the current measured by the wire scanner OWS-30 on the position

of the scanner wire, where the position 0 of the scanner wire corresponds to the center of the ion beam. In the radial profile of the ion beam, a certain asymmetry of the ion beam is seen, and it is seen that with a decrease in the pressure of the residual gas the beam increases in size. Making averaging with respect to the center of the beam and carrying out the Abelian transformation, we obtain the radial distribution of the ion beam current, which is shown in Fig. 6b. It can be seen that the ion beam is annular, as the pressure of the residual gas decreases its size increases and it becomes more hollow.

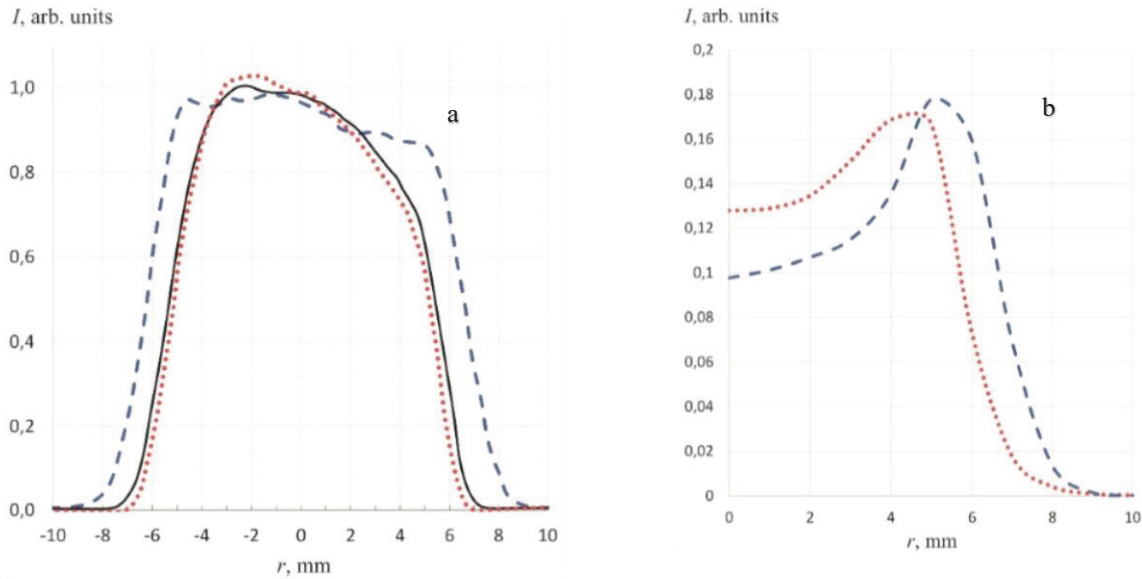


FIGURE 6. Profiles of chordal measurements of the ion current (a) and reconstructed radial distributions of the ion current (b) at different values of residual gas pressure (2.5 mPa - dashed line, 10 mPa - solid line, 20 mPa - dotted line).

In order to understand the reason for the beam injected into the accelerator being more annular rather than Gaussian, the phase portrait of the beam was measured using a scanner and a movable diaphragm. Since profilometer has 2 wires, there are 2 peaks at the measured profile. The width of the peaks corresponds to the transverse momentum of the part of the beam and distance between peaks corresponds to the coordinates of the part of the beam. For reducing the beam size in the diaphragm region, the current of the magnetic lenses was increased from 54 to 65 A. The diaphragm step was 0.5 mm. The results are shown in Fig. 7. To calculate the beam emittance, the data of the smoothed curves are approximated for the wire coordinates (for each diaphragm position), and the current in the region bounded by these coordinates and outside this region are determined. The invariant normalized emittance of the beam, in which $2/3$ of the current is concentrated, amounted to 1.7 ± 0.1 mm mrad (for the 2 mA beam). This emittance is an order of magnitude lower than the acceptance value of the accelerator stripping tube, but clearly visible in Fig. 7b, the difference between the phase portrait of the beam and the ellipse can lead to beam losses in the accelerating path. This curvature of the portrait is due to the spherical aberration of the magnetic lenses caused by the large initial divergence of the generated ion beam. The improvement in the quality of the ion beam injected into the accelerator and, accordingly, the reduction in the ion losses during acceleration requires lessening the effect produced by spherical aberrations of the lenses, which is possible either by increasing the aperture of the lenses or by decreasing the size of the ion beam in the lens region. Also, to prevent the heating of the diaphragms of the electrodes it is necessary to cool the diaphragm of the first electrode which is technically feasible.

Two Hikvision camcorders were installed in the accelerator, which detected the radiation produced by the interaction of the ion beam with the residual and stripping gases, and the radiation from the heated diaphragm of the first accelerating electrode (potential +166 kV). Figure 8 shows the image from the video camera, on which the ion beam is visible in blue, and the diaphragm is red. The image from the video cameras made it possible to monitor the position of the ion beam in two directions in real time. The implementation of optical diagnostics of the beam position in the diaphragm of the first accelerating electrode made it possible to improve the stability of the accelerator operation.

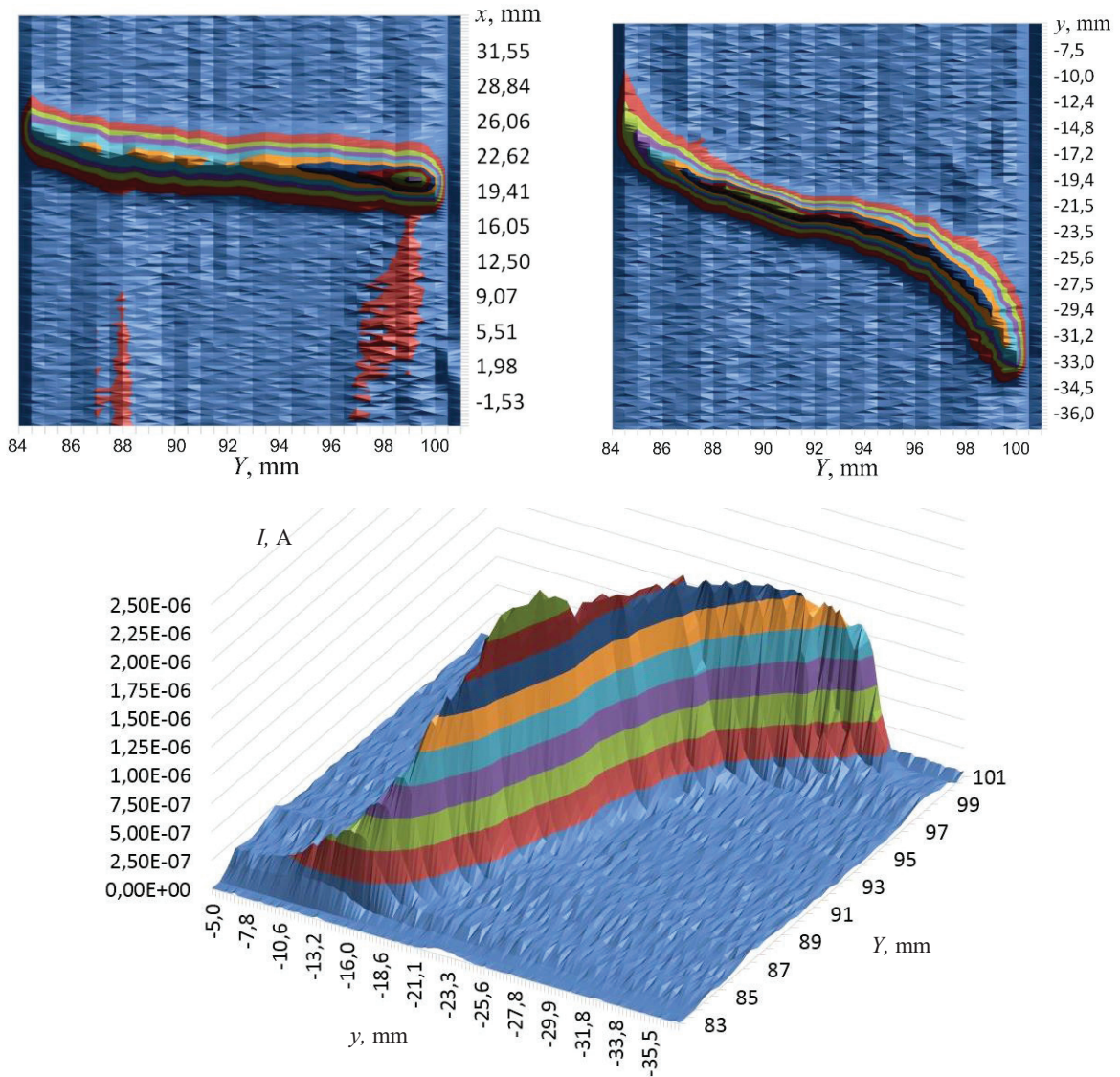


FIGURE 7. The beam phase portrait in the azimuthal (left), radial (right) directions and 3-D view (bottom). On the abscissa axis, the values of the diaphragm aperture position Y (along the y axis, see Fig. 2) are plotted, along the ordinate axis - the positions of the scanner wires (x or y , see Fig. 2). For each position of the diaphragm aperture moved by steps of 0.5 mm, distributions of the current measured by the scanner (characteristic values of the current - 10^{-7} - 10^{-6} A) are constructed. The signal amplitude is presented by uniform partitioning into 10 ranges from the maximum value; the ranges are shown by the same color.

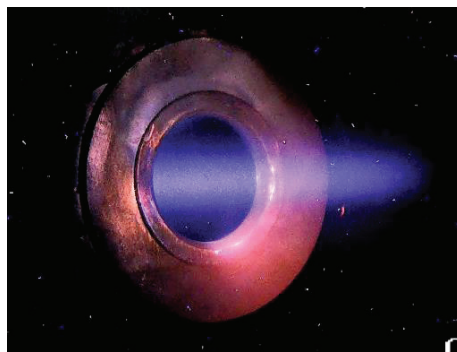


FIGURE 8. The camera image of the ion beam pass through the diaphragm.

SUMMARY

The OWS-30 wire scanner (D-Pace, Canada) was used to measure the dependence of the profile and current of negative hydrogen ion beam injected into a vacuum-insulated tandem accelerator on the residual gas pressure. The phase portrait of the beam was measured by means of a scanner and a movable diaphragm. The effect of a space charge and aberrations of a focusing magnetic lens on a beam of negative hydrogen ions is discovered. It has been established that the beam profile is close to annular and the maximum beam current density is attained at an intermediate pressure of the residual gas in the transport channel equal to 7.5 mPa. The value of the normalized beam emittance is determined; its value is 1.7 ± 0.1 mm mrad.

The change in beam focusing mode and the implementation of optical diagnostics of the beam position in the diaphragm of the first accelerating electrode made it possible to significantly improve the stability of the accelerator operation at high current of the proton beam, up to 6.7 mA.

This study was carried out with a grant from the Russian Science Foundation (Project No. 14-32-00006-P) with the support of the Budker Institute of Nuclear Physics and Novosibirsk State University.

REFERENCES

1. B. Bayanov, V. Belov, E. Bender, M. Bokhovko, G. Dimov, V. Kononov, O. Kononov, N. Kuksanov, V. Palchikov, V. Pivovarov, R. Salimov, G. Silvestrov, A. Skrinsky, S. Taskaev. "Accelerator based neutron source for the neutron-capture and fast neutron therapy at hospital", *Nuclear Instr. and Methods in Physics Research, A* **413**/2-3, 397 (1998). DOI: 10.1016/S0168-9002(98)00425-2
2. S. Taskaev. "Accelerator based epithermal neutron source". *Physics of Particles and Nuclei*, **46**, 956 (2015). DOI: 10.1134/S1063779615060064
3. W. Sauerwein, A. Wittig, R. Moss, Y. Nakagawa (editors). *Neutron Capture Therapy: Principles and Applications*. (Springer, 2012), p. 553.
4. A. A. Ivanov, D. Kasatov, A. Koshkarev *et al.*, *Technical Physics Letters*, **42**, 607 (2016). DOI: 10.1134/S1063785016060225.
5. B. Bayanov, V. Belov, S. Taskaev. "Neutron producing target for accelerator based neutron capture therapy". *Journal of Physics* **41**, 460 (2006). DOI: 10.1088/1742-6596/41/1/051
6. <http://www.d-pace.com/?e=70>
7. E. Sokolova, D. Kasatov, Ya. Kolesnikov, A. Koshkarev, A. Kuznetsov, A. Makarov, I. Shchudlo, I. Sorokin, S. Taskaev. "Measurement of the Ion Beam Profile with the D-Pace Wire Scanner". Proceedings of the XXV Russian Particle Accelerator Conference (RuPAC 2016), St. Petersburg, Russia, THPSC069 (2016).
8. T. Bykov, Ia. Kolesnikov, A. Makarov, I. Shchudlo, E. Sokolova, S. Taskaev. "Measurement of the negative ion beam with D-Pace's OWS-30 Wire Scanner", *these proceedings*.